

Lack of low-density cosmic-ray tracks*

A. F. Clark, H. F. Finn, N. E. Hansen, and D. E. Smith

Lawrence Livermore Laboratory, University of California, Livermore, California 94550

(Received 1 March 1973; revised manuscript received 22 April 1974)

A diligent search for low-density (quark) tracks in cloud-chamber pictures of cosmic rays has been negative. The flux of fractionally charged particles in extensive air showers (EAS) is estimated, at a 90% confidence level, to be less than $2 \times 10^{-11} \text{ cm}^{-2} \text{ sr}^{-1} \text{ sec}^{-1}$ for particles having a charge of $\frac{2}{3}e$, less than 8×10^{-11} for $\frac{1}{3}e$, less than 7×10^{-10} for $\frac{1}{4}e$, and less than 1×10^{-7} for $\frac{1}{6}e$, where e is the charge on an electron. The chambers were triggered by EAS about once an hour; the ions were allowed to diffuse so that individual droplets could be counted; the positive- and negative-ion columns were separated in an electric field so that the timing of the tracks was measured and the proper operation of the cloud chamber monitored. Individual droplets were counted "by hand" (looking in microscopes) and by automated methods. Artificial low-density tracks were superimposed on regular pictures to train the scanners and to measure their efficiency. 200 000 stereo picture pairs containing 10^6 cosmic-ray tracks have been scanned for quark tracks; none has been found.

I. INTRODUCTION

All the very-high-energy atom-smashing machines have been used to try to create and observe quarks (unsuccessfully so far). Quarks have been sought on land, in the sea, and in the air (cosmic rays).¹

McCusker and Cairns² felt that the cosmic-ray searches had not been thorough enough. They argued that quarks are likely to be created only in very-high-energy collisions (otherwise people should have found them in the accelerator experiments). A very-high-energy cosmic ray is accompanied by a shower of particles called an extensive air shower (EAS). The previous cosmic-ray searches had looked for single unaccompanied particles with low ionization; however, quarks might occur only near or in the core of an EAS where there are many simultaneous particles close together; these other particles will produce extra ionization in the detector, thus masking the presence of the quark with its low ionization.

In the fall of 1969 McCusker and Cairns² announced the discovery of 5 low-density tracks in pictures of cloud chambers triggered by EAS's. Such a discovery was so important that we have tried to verify their findings.³

For this cloud-chamber investigation a quark is defined as a particle which behaves in a normal fashion in a cloud chamber except that its charge is $\pm\frac{2}{3}e$ or $\pm\frac{1}{3}e$, where e is the charge of an electron. The velocity of the particles is expected to be relativistic so that the ionization will be roughly independent of velocity, and the tracks should be straight. Thus, the ionization on quark tracks relative to other cosmic-ray tracks would average $\frac{4}{9}$ and $\frac{1}{9}$ respectively for $\frac{2}{3}e$ - and $\frac{1}{3}e$ -type quarks. Further, a quark is assumed to exist for a time

long enough to make a track in the cloud chamber.

In a nuclear interaction in the atmosphere, conservation of charge implies that some fractional charge should still exist after the interaction; particles with such charges should continue on down with the EAS. It is possible, but seems less likely, that high-energy interactions would result in particles with charges of $\frac{4}{3}e$, $\frac{5}{3}e$, etc. Our cloud chamber search would not differentiate such particles from slowly traveling protons producing heavy ionization.

The EAS's we observed were typically initiated by primary cosmic rays having an energy of 10^{15} eV or more; Monte Carlo simulations of such showers indicate that many particles with energies of 10^{13} eV and more will persist down to sea level. Therefore, there should be adequate opportunity for the creation of quarks in the lower atmosphere even if quarks have tens of GeV rest mass. Thus, if the quark's lifetime is reasonably long, some quarks should exist in cosmic-ray showers at sea level. (Our experiment was performed at 180 m.)

A cloud chamber seems an ideal detector to sort out a low-density track in the midst of a high flux of particles. A cloud chamber is especially suited to a search for poorly understood events because pictures of the event can be examined and re-examined in great detail. There is a very large amount of information in one track: The positions and distribution in space of about 500 droplets and details of companion tracks in the same picture can be examined and compared with each other. As will be explained later, we examined the positive- and negative-ion columns, the "blobbiness" along the track, the amount of separation of individual droplets due to diffusion, and, of course, the number of droplets per cm.

McCusker and Cairns² triggered their cloud chambers from a simple EAS triple-coincidence counter set; we did the same. We naturally tried to improve on their early work. They took stereo pictures; we took larger fourfold stereopictures. We monitored the performance of our cloud chambers by measuring the development of droplets on negative ions. They scanned for low-density tracks. We scanned with excellent optics; we checked, educated, and calibrated our scanners with artificial low-density tracks. They counted drops (aggregates of individual droplets); we counted individual droplets corresponding to single ions. We counted in a variety of ways including automated machine counting. They found 5 candidates in 60 000 cosmic-ray tracks. We have scanned 10^6 cosmic-ray tracks, and have no candidates.

Pictures were all scanned for low-density tracks by scanners using enlargers adapted to project 2 stereo views side by side. All "interesting" tracks were cataloged, i.e., prints were made of all tracks thought to be low-density; these tracks were examined in detail, including droplet counting of the original film. Some of the film was separately rescanned in order to catalog representative normal tracks. Cataloged tracks were then measured to obtain the space position and length of the tracks. Many of these tracks were read with an automated densitometer, the programmable film reader (PFR). Computer codes analyzed the film density profiles and found the droplets along the tracks. The computer code outputs were edited track by track to check the automated results. Finally, histograms were made of the numbers of tracks vs their droplet densities. Low-droplet-count tracks were re-evaluated for possible quark candidacy.

The organization of the paper is indicated in the following outline.

II. EXPERIMENTAL APPARATUS

- A. Cloud chambers and associated equipment
- B. Triggering system
- C. Optics and scanning equipment

III. EXPERIMENTAL PROCEDURES

- A. Scanning procedures
- B. Droplet counting
 - 1. Hand counting
 - 2. Computer counting
- C. Blob models
- D. Artificial tracks

- E. Calibrations using artificial tracks

IV. LOWER DENSITY TRACKS

- A. $\frac{1}{9}$ -ionization tracks
- B. Flat geometry
 - 1. $\frac{4}{9}$ -density tracks
 - 2. Foreshortening
 - 3. New scanning efficiencies
- C. Extremely low-density tracks

V. RESULTS AND DISCUSSION

- A. Limiting flux results
- B. Discussion
 - 1. Scanning efficiencies
 - 2. Quark candidates
 - 3. Limitations of the methods
- C. Other results
 - 1. Other histograms
 - 2. Magnetic monopoles
 - 3. Average energy loss per ion pair, w
 - 4. The variation in droplet counts due to the relativistic rise in ionization
 - 5. Droplet "weeping"
 - 6. Other cloud-chamber quark quests

II. EXPERIMENTAL APPARATUS

A. Cloud chambers and associated equipment

A maximum of 11 cloud chambers were used. These chambers were essentially identical^{3,4,5}: 44 cm in diameter, 23 cm deep, with a 10-cm illuminated beam through the middle of the glass or plastic cylinder. Xenon flash lamps were positioned on opposite sides of the cylinder. A 2.5-cm-thick flat glass plate formed one end of the cylinder, and a movable piston covered with black velvet filled the other end. The piston moved between stops, providing a fixed (but adjustable) volume expansion.

The chambers were normally filled with nitrogen gas at 1000 Torr and 20°C; however, argon, CO₂, and helium were employed in some experiments. The condensable vapor was about 65% ethyl alcohol and 35% water; this combination gave a particularly large increase in the ease of formation of droplets on positive ions as compared with negative ions.⁶

The expansion of the chamber was triggered by

an EAS and occurred slowly enough (about 80 msec) for the ions to diffuse and separate about 1 mm. The droplets were allowed to grow bigger for an additional 170 msec, at which time the flash lamps were fired and the film exposed. Droplets on individual ions could be seen and counted (see Figs. 1 and 2).

An elaborate set of grid wires was developed and used to maintain an axial clearing field of about 40 volts per cm which swept out miscellaneous old ions. When the cosmic-ray shower triggered the cloud chamber, the electric field was switched in direction and magnitude to 10 volts per cm at right angles to the viewing (axial) direction. This horizontal field separated the positive- and negative-ion columns into 2 parallel tracks about 4 mm apart. The separations and densities of the ion columns monitored the proper operation of the cloud chamber and permitted the identification of tracks created at the time of the trigger. "Early" tracks made wider, more diffuse ion columns, which were separated also in the axial direction; "late" tracks were narrow and had less separation between the positive and negative columns. Tracks early or late by more than 20 msec were identifiable as not simultaneous with the EAS.

When the negative-ion column had droplets developed on more than 15% of the ions, then the positive-ion column had developed droplets on all of the ions.⁶ Thus, the proper operating conditions of the chamber were checked, and counting the droplets in the positive-ion column gave the number of ion pairs created. Sixty ion pairs per cm was the average count for EAS particle tracks. The usual operating region ranged between 30% and 80% development of droplets in the negative-ion column. Increasing expansion ratios, i.e., increasing droplet development on negative ions, also increased the number of background droplets and made scanning and counting much more difficult.

The bottom of the cloud chamber was purposely kept slightly colder than the top in order to decrease convection, a primary cause of turbulence and crooked tracks (see Fig. 1).

Two slow expansions were commonly used after a fast expansion, in order to get rid of the background droplets. With effort and know-how the average single droplet background decreased to about 0.2 droplets/cm³ and was sometimes 0.03/cm³.

The thick (2.5 cm) flat viewing glass was kept slightly warmer than the rest of the chamber so that vapor would not condense on it and obscure the field of view.

Once a chamber was clean and operating proper-

ly, it would usually remain in good condition for months, with only minor adjustments of the expansion ratio, etc. However, some chambers leaked slightly; nitrogen was added about once a month, and liquid was added every few months as needed.

There were always some cloud chambers not in use: Grid wires were shorting out, or the experiment was being changed, etc. An average of 7 cloud chambers were in operating condition at any one time. One man spent most of his time just taking care of cloud chambers.

B. Triggering system

The triggering system was a simple threefold coincidence between counters about 2 m apart arranged in a horizontal plane. The sensitive area of the detectors was the same (115 cm²) as that of McCusker and Cairns.² The counters, 1.2-cm-thick plastic scintillators, were adjusted to trigger on pulses due to singly charged particles. Usually, 3 trigger systems were used to activate the cloud chambers. Chambers were positioned close together. The detectors were about 1.5 m above a typical chamber. A chamber was triggered when one of the triple-coincidence counters was directly above it, or alternatively when 2 counters about 1 m to one side and the third counter about 2 m farther away obtained a signal.

The shower particles passed through the roof of the building and varying amounts of Pb. The roof consisted of the equivalent of 4 g/cm² of "rock" and 4 g/cm² of "carbon," i.e., wood, etc. About half of the cloud chambers had Pb above them covering an area corresponding to an angle out to about 45° from the zenith. The triggering counters were on top of the Pb. Usually the Pb was 10 cm thick, but it was 20 cm thick in some cases. Ten cm of Pb decreased the number of shower tracks by about a factor of 3. Pb with about 6 g/cm² of Al beneath it decreased the track count by about another factor of 2, presumably owing to the transition effect in the lower-atomic-weight material. Some chambers were stacked 1 m above other cloud chambers; the bottom chambers had Pb 0.5 m above them as well as the extra iron, aluminum, and glass of the upper cloud chambers.

C. Optics and scanning equipment

Two xenon flash lamps were used, one on each side of the chamber, with plastic cylindrical lenses to give roughly parallel light into the chambers. The lamps were painted white on the sides which were not facing the chamber in order to increase the light directed through the lenses.

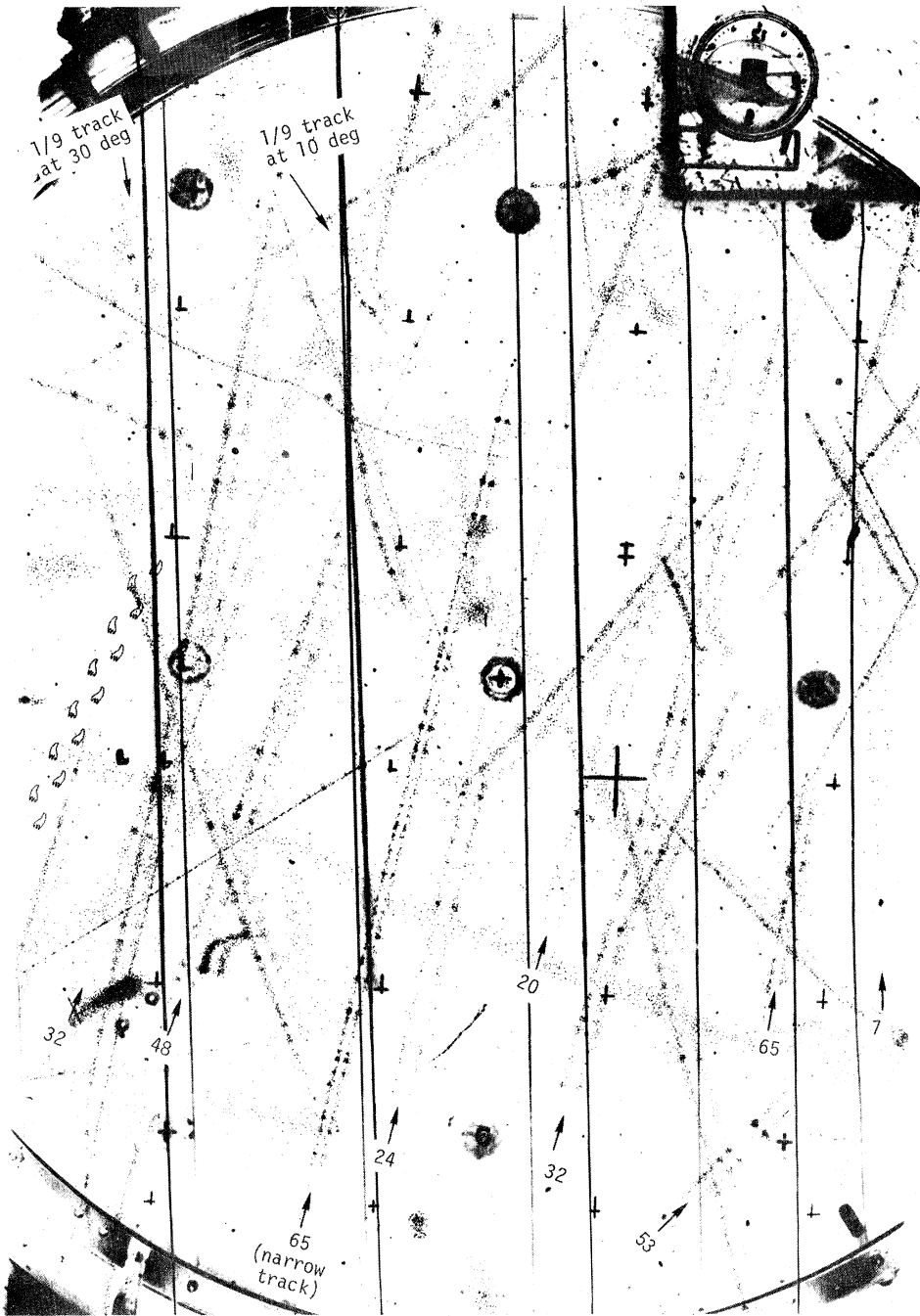


FIG. 1. An atypical photograph of a typical cloud chamber. The picture was taken looking approximately horizontally into a chamber; the zenith is at the top of the picture. There are 12 artificial tracks in this picture, indicating something of the variety of such tracks. The numbers in squares with arrows point along tracks made with a model to produce, on the average, the stated number of droplets per cm in the left-hand (positive) ion column. The 2 tracks in the upper left labeled $\frac{1}{9}$ are simulations of highly foreshortened tracks with $\frac{1}{9}$ normal density; the angles of the simulated $\frac{1}{9}$ -density tracks with the camera direction were 30° and 10° . The track at the left is also a "quark" track, i.e., it is formed with a droplet density of $\frac{1}{9}$ normal. This track should help convince people that one can be trained to detect certain kinds of tracks in the midst of much clutter. One can notice that the chamber was too hot (under-expanded) at the top because the negative (right-hand) ion columns of the real tracks are underdeveloped (almost absent), whereas the bottom of the cloud chamber was at the proper temperature with the negative columns about half as dense as the left-hand positive columns.

Flat mirrors on the top and bottom of the chambers increased the illumination about 50%. The lamps were excited with 500 joules stored in capacitors at 2000 volts. Four 35-mm Nikon cameras with automated backs and with excellent 55-mm lenses provided 6 possible stereopairs of pictures of each chamber, gave redundancy for camera failures, allowed simultaneous experiments with different film and camera settings, but most importantly permitted extremely detailed examination and evaluation of any quark candidate track. Candidate tracks partially obscured by other tracks and grid wires could be well understood by observing the tracks in different stereo views.

The separation between stereopairs of cameras was 16 cm (and $16\sqrt{2}$ cm). The cameras were placed 62 cm from the center on 6 of the cloud chambers and 72 cm from the center on the other 5 chambers. This variation in demagnification provided a check on the measurements of geometries and of numbers of droplets when the drop-

let images overlapped; the droplet images were the same size, but the different demagnification changed the amount of overlap. The lens apertures were commonly set at $f/11$ or $f/16$. Many experiments checked the results to be sure there were no variables which were not understood and taken into consideration.

A number of types of film were investigated; soon Linagraph Shellburst was chosen as being optimum with respect to sensitivity, acutance, and contrast. Later, with more light in the chambers, we changed to a reversal (positive) film, Eastman 2498, which made scanning a great deal easier. There was no question of returning to negative film even though the droplet diameter was about 25% larger (about 20 microns with 2498 film) and the density variations (in the reversal film) were very nonlinear (Fig. 2). The larger droplets implied considerably more overlap between neighboring images, and this increased the problem of counting individual droplets. However, the counting techniques improved so much that this was not the chief limitation.

The scanners examined a pair of side-by-side stereo images provided by 2 excellent enlargers modified for this work. These enlargers resolved 200 line pairs per mm with a magnification of about 10 to give dimensions approximately actual size. The chief problem in achieving good resolution was to get rid of mechanical vibrations.

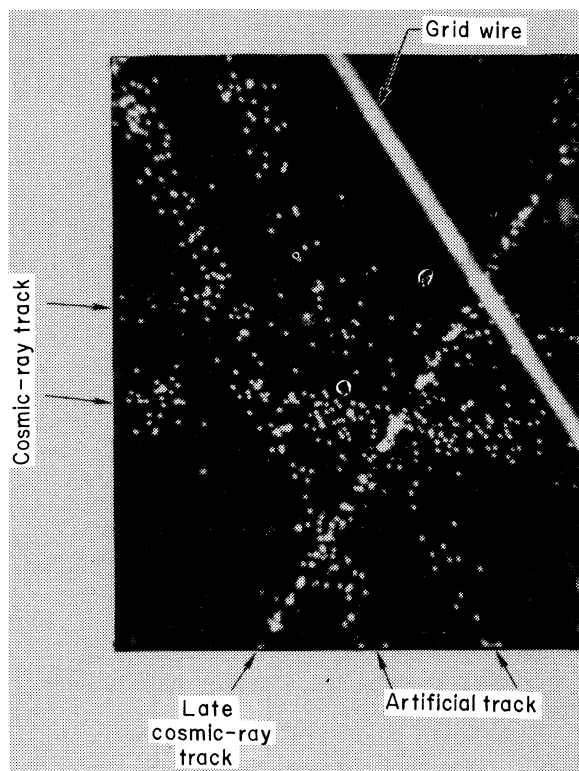


FIG. 2. Comparison of the droplets in normal and artificial tracks. The actual magnification from the reversal (2498) film is about $35\times$. The size of the droplets is determined by the resolution of the optics and the exposure of the film; the grid wire appears wide because it is so bright. The narrow single track arrived about 100 msec later than the cosmic-ray shower. Note the lack of background.

III. EXPERIMENTAL PROCEDURES

A. Scanning procedures

Numerous schemes were investigated to try to scan in a manner that would increase the likelihood of discovering low-density tracks. The scanner examined each view separately and could check that any track that looked interesting occurred properly displaced in both views. The most important improvement was the shift to reversal film; the scanner looked for objects of interest against a black background, instead of against a mottled bright background. The droplets stood out like very bright stars in the night sky; the difference is dramatic (see Fig. 2).

The scanners examined up and down and across the picture and looked at each frame in turn, checking the details of corresponding tracks and artifacts in the two views. An average scanning rate of 80 picture pairs per hour was achieved for the actual scanning effort. When interesting events were discovered, prints were made and cataloged. To relieve monotony, scanners did other work in addition to scanning. There was commonly only one scanner, but different people

worked at this job at different times. An excellent and basic part of the experiment involved artificial tracks used to educate and evaluate the scanner; this work will be detailed later.

A separate job involved looking at the same set of pictures to catalog ordinary tracks. Not all pictures were examined for this purpose, but enough tracks were cataloged to give a basis for measuring the variation in ionization of EAS tracks and to check the continuing proper operation of the chambers and the measuring systems. About 10% of all normal cosmic-ray tracks were cataloged. After a track was cataloged, marked prints and the film were sent to Lawrence Berkeley Laboratory (LBL). There, scanners and scanning tables were used to "skeletonize" the track; i.e., coordinates along the track in each of two views were measured. A computer program determined the space coordinates of the track, and the demagnification factor from actual space to film.

B. Droplet counting

1. Hand counting

A great deal of droplet counting has been done "by hand," looking through a microscope at original film. The earliest statistics were gathered from "hand" counting using a stereo microscope and original film. Three scanners were educated by Wilson Powell at LBL, and 2000 tracks in 3 categories were counted: (1) a representative set of cosmic-ray tracks, (2) quark candidates, and (3) a set of tracks from minimum-ionizing electrons.

These electrons were Compton electrons from Co^{60} γ rays; the tracks were photographed in a cloud chamber which had a magnetic field, and only tracks with a large radius of curvature were counted.

As the quality of the pictures (and cloud chambers) improved, it became easier to count tracks with an ordinary binocular microscope, and stereo counting was abandoned. There were, however, compromises in changing from stereo counting. Many areas included crossing tracks and other backgrounds which made it difficult or impossible to count except in stereo. On the other hand, it was easier, quicker, and more reproducible to count with an ordinary binocular microscope with a movable stage.

Some tracks were counted by hand from enlarged prints since that was so easy to do. However, such counts were usually low, and the number of droplets counted varied with the development of the print.

2. Computer counting

In spite of our good techniques, producing beautiful tracks, human counting was fallible; in fact, there seemed to be no way to prevent bias in counting. There were many decisions to be made as one counted along a track: One decided if various droplets were due to backgrounds or belonged to the track; one decided whether a particularly large drop (blob) was 1, 2, or 3 droplets, etc. If the track count seemed to be low, did the person compensate and count a few extra droplets, or did he eagerly try to make a small count? Since we needed to establish the distribution of track densities *without bias* in order to know if any observed low-density tracks were just statistical fluctuations, *automated counting* was needed. Codes were developed to deal in a completely reproducible way with each decision. The code starts and stops counting a fixed predetermined distance beyond each obstruction such as a crossing track, etc. The latest code modification starts and stops the counting a fixed distance inside the end points (which were picked out by the person cataloging the track), and thereby eliminates another source of bias. About 20 000 tracks of all kinds have been counted with the automated system.

Smith *et al.*⁷ described the system involving the 35-mm film, the LBL skeletonizing, the PFR digitizer, and 2 computer codes. The programmable film reader (PFR) measured the density of the film accurately every 5 μm across and along a track. The density data were processed by two computer codes. The first code found an average background density and the maximum density in a droplet, and defined the area of all objects with densities greater than background plus $\frac{2}{3}$ of the difference between the background and the maximum droplet density. This converted the PFR output of 64 shades of grey to a black and white picture of drops, grid wires, etc. This code adjusted for varying light levels along the length of the track and varying densities in the droplets. For instance, the droplet images sometimes changed gradually along the track from small intense ones to larger more diffuse spots.

The second code took the black and white information from the first code, located the track (the positive-ion column), measured the track width, and determined the average droplet size; the droplets which were beyond the track width were discarded as background. If there was too much local background, the background was identified as a crossing track and that portion of the track length was discarded; similarly, that portion of

a track which was too near a grid wire was discarded.

Early results had about 75% rejection by human editors; more recently with improved pictures, reversal film, improved codes, and considerably stiffer criteria for track acceptance for cataloging, the rejection rate was 10 to 15%. There was at no time an apparent bias as to which tracks (high or low density) were rejected. The accepted tracks were assembled for analysis into various histograms.

C. Blob models

The chief reason for the interest in the "blobbiness" of tracks was the need to develop "realistic" artificial quark tracks (see Figs. 1 and 2). The energy transferred to the secondary electrons varies roughly as the Rutherford cross section; i.e., the probability of a given energy being transferred to such electrons varies inversely as the square of this energy. Secondary electrons with energies up to about 10 keV travel negligible distances, but nevertheless create about one ion pair for each 34-eV energy loss. Such a local area with a high density of droplets is called a blob. As is commonly done when counting droplets in cloud chambers, we introduced a blob cutoff; we discarded portions of tracks containing a blob of more than 30 droplets in the positive-ion column. More specifically, if the number of droplets along a portion of the length of the track equal to the track width contained 30 droplets more than the average droplet count in such a length of track, then the computer analysis discarded that section of track. Blobs larger than the cutoff size are called "big blobs."

We postulated that the probability of producing a given number of ion pairs (n) in a primary interaction was inversely proportional to n^2 . Thus we assumed that the probability of producing 2 ion pairs from a primary interaction was $\frac{1}{4}$ the probability of producing a single ion pair, and that the relative probability of producing n ion pairs was $1/n^2$. One assumption for this model was that the Rutherford-type cross section holds down to energies low enough to make a single ion pair, and that the average energy to produce an ion pair is independent of the energy of the ionizing particle.

Artificial tracks were made from this model, using blobs of all sizes out to $n=300$. A code was developed to generate the random primary interactions; it then allowed the ions to diffuse to a Gaussian spacing, and calculated the two-dimensional projection of the ion positions. An automated drafting machine made spots on a plastic sheet corresponding to the projection of the ion

positions. On examining these tracks, one could see that the track had too many blobs. For each 20-cm track length there was about an average of 9 "big blobs," i.e., blobs with more than 30 droplets.

The model was then modified to have 4 times as many single ion pairs as before; i.e., the relative frequency of primary interactions producing blobs of size n is $1/n^2$ except for $n=1$, where the frequency is 4, not 1. The mean free path for primary ionizations was then renormalized to again give the measured 60 droplets/cm.

This model produced about 2.7 "big blobs" per 20 cm. This compared with our measured (2.5 ± 0.2) big blobs per 20 cm from computer-counted tracks, using the same criteria for big blobs.

Using Berger's⁸ restricted-energy-loss calculations for electrons, and assuming, again, the same average energy loss per ion pair, the predicted number of big blobs is 2.5 per 20 cm of track length.

Our model reproduced the experimental width of the histogram of tracks vs droplet density; i.e., the model gave the proper statistical fluctuation in the number of droplets per cm. The experimental standard deviation σ was not \sqrt{N} (where N is the number of droplets in a track) as it would be if each droplet were due to a statistically independent event. Instead, σ was about $\sqrt{4N}$ because of the "blobbiness"—the droplets are not all statistically independent.

D. Artificial tracks⁹

The artificial tracks were a most necessary and fruitful part of the effort. The scanners were looking for kinds of tracks which (in retrospect) were not there; at least, we knew that such tracks would be very rare. How could one be sure that a scanner would not miss such tracks? A verifiable solution was to put artificial tracks (of the appropriate droplet density and blobbiness) on the pictures which were to be scanned.

Double exposures with artificial tracks were made on a small number of more or less random pictures, and the scanners were expected to find these tracks in the normal scanning process. This procedure was very valuable: (1) It led to a measure of the scanning efficiency; (2) it taught the scanners what to look for, and they thus improved their scanning efficiency a great deal; (3) it provided artificial tracks which were "carrots"; the scanners did find interesting tracks every day or so, and did not get careless or bored; and (4) it led to a sufficiently detailed knowledge of the tracks so that a calibration of the overlap problem was obtained.^{7,9}

The artificial tracks became faithful duplicates of real tracks except for the purposeful decrease in average droplet density. Appropriate discussions with the scanners continued throughout the program to check that there were no tell-tale features to trigger the scanner's attention; for instance, the need for slightly curved tracks (1.7 m radius) was discovered by talking to the scanner while we were developing the simulation with almost-normal-density tracks. For the really low-density tracks the problem was to get the scanner to see the track at all. If he did see it, his interest was certain to be aroused. He needed to be educated to look for the right kind of low-density tracks by finding "realistic" artificial tracks.

The artificial tracks made with this model were so realistic that people could not tell the difference from real tracks, and scanners did not discover the best full-density artificial tracks. Having arrived at a good simulation of real tracks, we could then have confidence in our model for lower-density tracks: $\frac{4}{9}$, $\frac{1}{9}$, etc.; the established mean free path for primary interactions was increased by $\frac{9}{4}$, 9, etc. The blobs were separated correspondingly more, but the ratio of blobs to total droplets was preserved. We believe that this is the way fractionally charged particles would interact. The scanners became conditioned to looking for particular kinds of events to the exclusion of grid wires, low-energy "wiggly" electron tracks, old diffuse tracks, etc.

The efficiency of the scanners was measured with artificial tracks as a function of many variables: time, different density tracks, tracks at various angles (in 3 dimensions), different cloud chambers, etc.

E. Calibrations using artificial tracks

The artificial tracks proved very useful for other purposes. Detailed comparison of droplet counting could be made, revealing all the inconsistencies between the original artificial track with its constructed droplets and the counting of its double exposure as done both by hand and by computer codes. On such a basis the hand counting was discovered to be 15% low; the computer counting was renormalized with about 4% change to count correctly artificial tracks at 60 droplets/cm.

With the computer the reproducibility of counting the droplets in a given track was 3%; the accuracy per track, as determined by the artificial tracks, was about 8%. The average count of 35 tracks with densities between 52 and 70 droplets per cm was 0.5% low.^{7,9} At 32 droplets/cm the codes ap-

peared to be counting accurately; at 25 droplets/cm they counted perhaps 5% low. At densities of 90 to 100 droplets per cm the codes counted 0-5% low because of the extra overlap between droplets which was not properly compensated for at such high densities.

With such good codes one could expect the histograms of droplet densities to be quite unbiased; the codes were counting correctly throughout the range of densities of normal cosmic-ray tracks.

Details of the blob model were checked with the aid of the artificial tracks. The tracks were monitored for blobbiness and, as mentioned before, changes were made to make fewer blobs and thus to decrease the statistical fluctuations of the track counts. The standard deviation σ changed from $\sqrt{7N}$ to $\sqrt{4N}$, which now agreed with the widths of the experimental histograms.

IV. LOWER-DENSITY TRACKS

A. $\frac{1}{9}$ -ionization tracks

It gradually became apparent that the flux of $\frac{2}{3}e$ quarks was much less than we had hoped. However, no search for quarks is really complete unless one looks also for the $\frac{1}{3}e$ types. Even if all types were generated in cosmic-ray collisions, it is possible that some kinds would be more stable than the others and that $\frac{2}{3}e$ quarks would change, with further interactions (or just decay), into $\frac{1}{3}e$ types with the emission of other unit-charge products.

We therefore tried very hard to improve our techniques sufficiently to be able to look for $\frac{1}{9}$ -density tracks. We tried higher pressures and higher-density gases: CO₂ and Ar. To get lower backgrounds we scrubbed the cloud chambers, increased the illumination, and decreased the diffuse light by using less liquid (less condensation on the cylindrical windows). Temperature regulation was also improved. The most noticeable improvement came from increasing the minimum time delay between triggers from 10 to 15 and then to 20 minutes.

Without telling the scanner, we made up and put $\frac{1}{9}$ -density artificial tracks on the film, and the scanner found them. The scanner was now looking for (and finding) both $\frac{4}{9}$ - and $\frac{1}{9}$ -density tracks. While the search for $\frac{4}{9}$ -density tracks was continuing, the scanner was gradually educated to increase his efficiency in discovering $\frac{1}{9}$ -density tracks.

The scanning efficiency for $\frac{1}{9}$ -density tracks in chambers with a long dimension vertical leveled out at about 50%. It was greater than 50% for the cloud chambers under 10 cm of Pb, but was not

measured carefully. We know it was not 100% because about 10% of the artificial tracks were obscured by grids and other tracks.

B. Flat geometry

With an adequate scanning efficiency and the emphasis now on looking for $\frac{1}{3}e$, we turned 6 cloud chambers on their sides, with the long dimensions (diameters) horizontal, and the cameras looking down from on top. The advantages of the flat geometry were (1) that there was more area of intercepted flux by about a factor of 2, since most of the flux came from near the vertical; (2) these steep angles implied a great deal of foreshortening of the track picture with the concomitant increase in apparent droplet density; this made it easier for the scanner to discover low-density tracks (most tracks were still adequately long to be seen readily); finite scanning efficiencies were obtained for even $\frac{1}{36}$ -normal-density tracks; (3) these shorter tracks permitted adequate scanning in denser showers; the tracks did not obscure each other as much since they were short; (4) these variations of experimental conditions represented valuable checks on possible errors.

1. $\frac{4}{9}$ -density tracks

The efficiency for detecting $\frac{4}{9}$ -normal-density tracks varied from an assumed zero (i.e., unmeasured) for a part of the time to 30% when the scanner became much more knowledgeable and sophisticated. However, the scanning was finite, and the limiting flux number from this part of the search alone is $10^{-8} \text{ cm}^{-2} \text{ sec}^{-1} \text{ sr}^{-1}$, which represented a check on the other work.

2. Foreshortening

Most of the tracks in the flat geometry were highly foreshortened; they passed through the entire illuminated depth and had an apparent length closely proportional to their zenith angle, which implied an apparent droplet density inversely proportional to their length. Such artificial tracks (labeled $\frac{1}{9}$) are shown at the top of Fig. 1. The label also gives the "zenith" angles (10° and 30°); these angles are, more precisely, the angles with the camera direction.

3. New scanning efficiencies

Foreshortened artificial low-density tracks were made of appropriately varying lengths and densities. The frequency with which the different kinds were used to educate and check the scanner

was varied in a manner roughly proportional to the expected cosmic-ray flux at such angles; e.g., more tracks were made to simulate angles of about 20° than other angles. There were relatively few tracks near 10° because of the small solid angle; there were fewer tracks beyond 30° , since most of the EAS tracks occurred at smaller zenith angles due to atmospheric absorption. These tracks were placed at various angles and positions on the cloud chambers. The negative columns were displaced relative to the positive columns since the tracks were not at right angles to the electric separating fields (see Figs. 1 and 2).

However, not all tracks could be scanned effectively. One continual requirement was that a negative- as well as a positive-ion column be identified. Since the separating field pulled the ions in a given horizontal direction, there was no apparent separation if the track itself lined up in that direction, and the negative column appeared on top of the positive column instead of beside it. In the original geometry the separating field was horizontal, and, since very few tracks had angles greater than 45° with the zenith, there was no solid-angle exclusion introduced by the requirement of separated tracks. We have tried unsuccessfully to scan for unseparated tracks, but have needed the criterion of separated columns in order to be sure of our track identification. The scanner was asked to find only tracks with separated and identifiable positive- and negative-ion columns; otherwise he was not able to scan effectively and rapidly. We estimated that the criterion requiring separated columns *in at least one view* decreased the solid angle scanned by about 30%.

When a cosmic ray was coincident with the optic axis of one camera, it had an angle of 14° in the other stereo view, and was easily visible with a length of about 2 cm. For tracks of a nominal $\frac{1}{9}$ density, the scanner was more likely to miss tracks at angles greater than 35° because the apparent track density was so low.

In order to obtain an over-all average efficiency, the measured scanning efficiency at various angles was weighted by the known dependence of EAS on zenith angles. Further, the efficiency so derived was a function of time (i.e., of the scanner's education), and the over-all efficiency was weighted by the amount of film scanned and the efficiency of the scanner during that period. This average efficiency was probably an underestimate because it did not take into account the smaller but finite contributions of other people checking the film. A large fraction of the film was examined by people other than the regular

quark scanner; they cataloged tracks and checked the daily operation of the chambers. These people were educated scanners and also looked for quarks; they found the artificial tracks quite regularly. The actual efficiency may be higher because the solid-angle calculation did not allow for the increase in efficiency in one or the other picture due to the angle giving a more visible track in that view.

C. Extremely low-density tracks

We first used some $\frac{1}{12}$ -density tracks in order to be sure that the efficiency did not drop off suddenly at $\frac{1}{9}$ normal density. If such had been the case, then the statistical fluctuations in the $\frac{1}{9}$ -density quark tracks would have decreased the real efficiency: Some (short) tracks would average, for instance, $\frac{1}{12}$ density, etc. Further, such training improved the scanner's ability to see $\frac{1}{9}$ -density tracks. The scanner had a decreasing but finite efficiency out to $\frac{1}{36}$ -normal-density tracks (corresponding to $\frac{1}{8}e$) in the foreshortened geometry. Again, an educational program was necessary to train the scanner to see such tracks, but once he was trained, such tracks "jumped out of the picture at you." Those who examined much film found this phenomenon happening.

Artificial tracks were made up corresponding to space track densities of $\frac{1}{12}$, $\frac{1}{18}$, $\frac{1}{36}$ normal densities; i.e., tracks were made by the computer codes to average such densities. Twenty-cm lengths of nominal densities $\frac{1}{12}$ and $\frac{1}{18}$ were selected as being not too blobby; then short sections were chosen at random to be made up into artificial double exposures. Only 1 out of 40 selected tracks had a blob with over 30 droplets; statistically there should have been 3 such "big blobs."

The scanner could not find the first $\frac{1}{36}$ -density tracks. Therefore, unlike all the other artificial low-density tracks, these tracks were especially chosen *with* a big blob someplace along their length, since big blobs were highly visible.

V. RESULTS AND DISCUSSION

A. Limiting flux results

No adequately defensible quark-candidate track has been discovered during the scanning of 10^6 tracks from extensive air showers, i.e., during the scanning of 200 000 pairs of photographs.

About 170 000 stereo pairs of pictures (about 20 pictures per chamber day) were scanned for $\frac{4}{9}$ -density tracks. Over $\frac{1}{2}$ of these were also scanned for $\frac{1}{9}$ -density tracks. About 35 000 picture pairs with foreshortened tracks were scanned for $\frac{1}{9}$ -density tracks; of these about 15 000 were also scanned with measured efficiencies for $\frac{4}{9}$, $\frac{1}{12}$, and $\frac{1}{18}$ densities, and about 4000 for $\frac{1}{36}$ -density tracks.

The principal conclusions of this work are expressed as an upper flux limit for the existence of quarklike tracks in cloud-chamber pictures of EAS's.

The pictures scanned represented a certain area which was exposed to the cosmic-ray flux of EAS's during the time that the chambers were ready and waiting for an EAS trigger. Thus, the limiting flux is the inverse of the product of the effective area, the solid angle to which the detector was sensitive, the total available time, and the efficiency of the scanner in detecting the interesting tracks.

Table I lists the results. The area used is a straightforward number, the projected horizontal area of the scanned volume of a cloud chamber. For the original geometry (with the cylindrical axis of the chambers horizontal) the horizontal cross section of the illuminated volume was multiplied by 2 because the average visible length of tracks was *less* than half the vertical dimension of the chamber; measurements showed that such tracks had a typical EAS zenith-angle distribution. Thus, a chamber could be considered as being 2 detectors, one on top of the other.

The solid angle used (0.67 sr) is that for EAS's transmitted by the atmosphere. Instead of using

TABLE I. Track densities are given in fractions of the average density (60 droplets/cm) of shower tracks in 1000 Torr N_2 . The maximum scanning efficiency for $\frac{1}{36}$ -density tracks with "big blobs" was 20%; big blobs should occur 3% of the time. For comparison with other experiments, see Ref. 1 and Sec. VC6 of the text.

| Track density relative to normal tracks | $\frac{4}{9}$ | $\frac{1}{9}$ | $\frac{1}{12}$ | $\frac{1}{18}$ | $\frac{1}{36}$ |
|--|---------------------|---------------------|---------------------|---------------------|--------------------|
| Maximum scanning efficiency | 80% | 65% | 45% | 30% | 0.6% |
| Average scanning efficiency | 70% | 50% | 25% | 15% | 0.3% |
| Limiting flux: $\text{cm}^{-2} \text{sec}^{-1} \text{sr}^{-1}$ | 2×10^{-11} | 8×10^{-11} | 5×10^{-10} | 7×10^{-10} | 1×10^{-7} |

0.67 sr for $\frac{4}{9}$ - and $\frac{1}{9}$ -density tracks, one could use the total scanned solid angle of the cloud chamber. The solid angle would be about 1.84 sr, including tracks out to 45° to the zenith. The scanners looked for and recorded tracks out to zenith angles of 60° , but their efficiencies were lower beyond 45° . The flux limits per sr would be decreased by $1.84/0.67$, e.g., to 7×10^{-12} for $\frac{4}{9}$ density and 3×10^{-11} for $\frac{1}{9}$ density. However, no extremely low-density artificial tracks were discovered with zenith angles greater than 35° ; such tracks were difficult to distinguish from chamber background droplets. One could then multiply the solid angle by $1.0/0.67$ but not more.

B. Discussion

1. Scanning efficiencies

The numbers in Table I represent actual scanned limits multiplied by the usual factor of 2.3 to give the nominal 90% confidence level for the statistics of the answer. The areas and times are relatively accurate; however, some of the efficiencies used to arrive at the final results have errors considerably more than 10%. For instance, some of the efficiencies, which have been assumed zero, were actually quite finite.

Certainly the dominant errors are in the scanning efficiencies. The scanners' efficiencies varied with time, their indoctrination, with types of tracks, with kind of film, the condition of the cloud chambers, etc. The program of artificial tracks was continually developed with the main purpose of measuring and increasing these efficiencies. The scanners were never aware when to expect an artificial track (except for the very earliest tracks, which were not used to compute the efficiencies).

A great deal of care has been taken to be sure there were no clues to the presence of an artificial track. This has been a main concern throughout the artificial track program. Everyone understands the problem, and we are confident that there is no major flaw in the measured efficiencies. The pattern of the scanners' ability increased in a reasonable way as a function of time. The scanners' efficiency has not been unbelievably high. The artificial tracks used were more difficult to discover than tracks that were either too blobby or too uniform in droplet density.

The scanners were shown the tracks they missed only during the brief training periods. In general, discussions of the problems and progress with the artificial tracks took place without the scanners' knowledge. They were praised for their work, but were kept in ignorance of the details of the experi-

mental artificial-track program.

The lower-density artificial-track program included 163 photographs of 24 different randomly selected sections of tracks; the scanner found the same section of a track an average of 3 times.

In Table I the efficiency for finding normal, non-blobby $\frac{1}{36}$ -density tracks is derived from the experimental scanning efficiency of 20% for tracks with big blobs. Using the measured average of 2.5 big blobs per 20 cm of normal track length, the probability that a 10-cm track of $\frac{1}{36}$ average density would have a big blob is 3%, so the efficiency numbers for the $\frac{1}{36}$ -density tracks were multiplied by 3% to give 0.6%.

2. Quark candidates

"Interesting" tracks. A large number of tracks and artifacts were tagged as "interesting." Most of these proved to be spurious, or not worth further consideration for various reasons. The most common mistakes were to "tag" a negative-ion column, or for the track to lack an identifying negative column. 395 real tracks were found to be interesting or exciting to somebody for some reason and could be droplet counted. All these tracks were considered quark candidates, and all were given very special treatment, including at least one droplet count. After detailed consideration, no track remained as a quark candidate, in spite of the fact that we were most interested in obtaining a positive result.

There were 3 categories of exciting tracks: (1) One type was the tracks made when the cloud chambers were not operating properly. These were the most difficult to understand. Sometimes the scanner looked at pictures he was not supposed to, when it was known that the cloud chambers were not at the proper temperature. The most difficult "track" to explain turned out to be 2 almost parallel tracks in an underexpanded (hot) chamber. (2) Very-low-density tracks ($\frac{1}{9}$ and less) were sometimes confused with parts of old background tracks, single blobs, and droplets which happened to form into a straight line. In such cases the redundancy of 4 cameras helped to show that the "track" was just a background blob, usually near the top or bottom of the illuminated volume. (3) Artificial tracks sometimes slipped through the system, and people got excited until it was determined that the track was not real.

3. Limitations of the methods

When the tracks were too close together, the negative column belonging to a particular positive column could not be identified. The maximum

fully scannable flux was about 500 tracks per m², with a decreasing but finite efficiency to about 5000 tracks per m². There were comparatively few photographs with high particle densities, and relatively few tracks were missed because of particularly high fluxes. The measured scanning efficiencies took this problem into account.

The statistical fluctuations in droplet densities were large enough so that a $\frac{4}{9}$ -density track was not improbable among all the tracks scanned. The histogram of the distribution of normal tracks vs average droplets per cm is quite broad (Fig. 3); we assumed $\frac{2}{3}e$ quark tracks would form a similar histogram with a peak at about $\frac{4}{9}$ the density of the normal peak and a standard deviation about $\frac{2}{3}$ that for the normal tracks. There were some tracks with a sufficiently low droplet count to correspond to a possible $\frac{4}{9}$ -normal-density track. All such tracks with densities of 40 per cm or less have been re-examined, but they have been substandard in at least one of many ways: foreshortened so that the count was low (i.e., too much overlap), poorly illuminated, out of focus, short so that the droplet statistics were inadequate, lacked contrast, near the edge of the

cloud chamber, etc. The histogram showed a rapid decrease of such tracks with decreasing droplet count. None of these low-density tracks warranted publication.

The number of tracks which had been droplet counted was estimated at 30 000 out of 10⁶ total. We do not understand the blobbiness of tracks well enough to predict statistically how many low-density quarklike tracks to expect; the histograms are not Gaussian but are sums of Poisson distributions. However, the experimental histogram indicated that there were about 1000 uncounted tracks which were within the expected variations of $\frac{4}{9}$ of the normal-droplet-count tracks. Why then did the scanners not discover these tracks? The scanners were "programmed" to find tracks that looked like the artificial tracks, and they learned to overlook most of the substandard tracks. They did find many light-substandard tracks. We do not claim that we would have found every quarklike track that was photographed. We do claim to have a measured efficiency and flux limit for finding tracks which are believed to be "realistic" quark tracks.

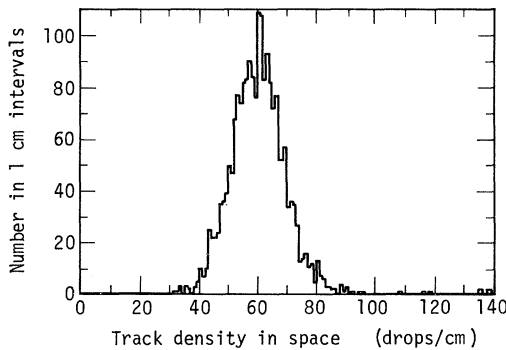
After 2 or 3 years of unsuccessful searching,

Track density distribution
N₂ 2498 film - background subtracted

2296 tracks were examined
2022 fit criteria
4 fit but were > 140/cm

Selection criteria
No. good drops 200 - 2000
Zenith angle 0 - 45
chambers not under lead
62 cm camera geometry

Density values
Average 59.9 Minimum 31.0
Variance 9.9 Median 60.0
Peak at 62 Maximum 138.0



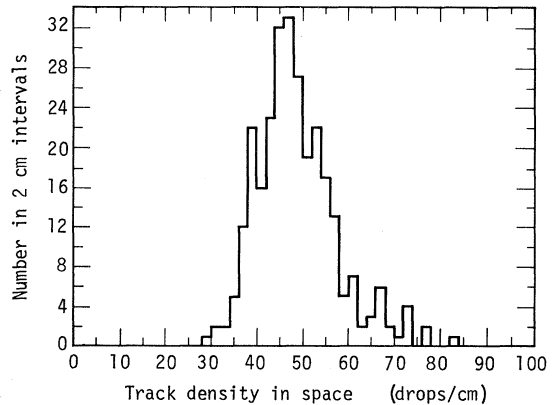
(a)

Track density distribution
N₂

282 tracks were examined
279 fit criteria
2 fit but were > 100/cm

Selection criteria
No. good drops 1 - 2000

Density values
Average 48.2 Minimum 29
Peak at 47 Median 47
Maximum 82



(b)

FIG. 3. Numbers of tracks vs droplet density per cm. (a) Histogram of EAS tracks from cloud chambers not under Pb, counted from reversal film. (b) Histogram of quark candidates counted by hand. 68 machine-counted tracks averaged 10% higher, and produced a similar histogram.

one wonders if we did not become blasé and overlook interesting tracks. The answer seems to be no. The scanner knew that he had an interesting continuing job if he could find a quark track and that he probably would no longer have a job if we did not succeed. As time went on, the experiment continued to improve and change, with new interesting problems and new achievements and goals. As the scanner improved and started looking for lower-density tracks, he kept finding new kinds of low-density background events which we examined in great detail to elucidate the newly discovered phenomena.

The finding of the $\frac{1}{36}$ -density tracks was bothered with background problems. The scanner frequently found chance alignments of a few droplets which had to be inspected with much care to determine that the droplets were due to a statistical fluctuation of droplet positions along an old diffuse short section of track. A short old single column sometimes showed a lack of droplets along a line down its length so that it looked like 2 separated columns, but this occurred in one view only, and a stereo viewing showed that the droplets were quite diffuse.

C. Other results

1. Other histograms

Many histograms such as Fig. 3 have been formed of the distribution of tracks of different densities vs gas, chamber, Pb over the chamber, time, film, chamber geometry, camera geometry, etc. In general, the differences were slight and could be rationalized adequately. A histogram of the distribution of tracks vs zenith angle θ was very close to a $\sin\theta\cos^3\theta$ curve, i.e., the distribution was proportional to the solid angle and the $\cos^3\theta$ attenuation factor for EAS's. This was another indication of the adequacy of our techniques.

2. Magnetic monopoles

The scanners were made aware of the possibility of finding magnetic monopoles, and we showed much interest in any high-density track discovered. Although one might expect a high scanning efficiency, it was not measured. High-density tracks were very rare, and none appeared sufficiently dense to be exciting. The tracks were most readily explained as breakup products of atomic nuclei; for instance, there was a "star" from an argon nucleus which captured a meson.

3. Average energy loss per ion pair w (Ref. 10)

There was no known measurement of w , the average energy loss per ion pair for "wet" gases; therefore, we measured accurately the relative amount of ionization in dry air vs that in a saturated gas corresponding to the cloud chamber mixture.¹⁰ No anomaly appeared; $w = 33.8 \pm 0.2$ eV per ion pair for our cloud chambers.

4. The variation in droplet counts due to the relativistic rise in ionization

The expected ionization of EAS tracks is a function of the energy distribution of the particles¹¹ and the variation in ionization with energy.¹² Some of the particles were highly relativistic with an average ionization about 1.4 times the minimum. The EAS particles included electrons with energies down close to the energy to produce minimum ionization (1.3 MeV). However, low-energy electron tracks were likely to be "wiggly" and therefore were discarded; the average cutoff due to multiple scattering was estimated to be 4 MeV. The percentage of low-energy electrons in the EAS was a function of the material just above the chambers because of the transition effect (a lack of equilibrium between production and attenuation of the radiations). Using a big-blob cutoff of 30 droplets, corresponding to a restricted energy loss of 1000 eV, and the energy loss results for electrons,^{8,10} the average count of our normal EAS tracks (Fig. 3) was 1.18 times the minimum ionization. The spectrum of Richards and Nordheim¹¹ gave an expected average 1.26 times the minimum. We attempted to construct a spectrum similar to that of Richards and Nordheim, allowing for a few percent of muons, and obtained a median electron energy of, very approximately, 10 MeV for our histogram. Further, we measured an increase in average droplet count for 120-MeV electrons of 1.39 times the minimum count, which agrees with theory¹²; we are skeptical of some of these experimental numbers and have not found time to verify them. However, our blob model gave the appropriate ratio⁸ of restricted energy loss to total energy loss for electrons.

5. Droplet "weeping"

A further refinement of the artificial tracks involved separating the droplets in the negative column more than in the positive column. When the negative column was not fully developed, it took longer for the ions to form sizable droplets and thus to stop drifting in the electric field. The droplets tended to "weep" in the direction of the

electric field. This phenomenon was particularly noticeable where there was a big blob, such that the local vapor density was decreased by all the other droplets which were growing. Then the ions migrated with the electric field into new regions where the vapor density was sufficient to permit droplet formation and growth. At lower vapor pressures, this effect was seen in the positive column also. Examination of narrow (late) tracks revealed ion motions that corresponded to time delays for droplet growth of the order of a microsecond.

6. Other cloud-chamber quark quests

McCusker's work triggered other cloud-chamber efforts. Hazen¹³ used a cloud chamber with an effective area of 0.15 m² and with horizontal Al and Pb plates, below which there were fewer tracks; thus, scanning of that part of the chamber was much easier. However, no measure of the scanning efficiency or scanner education was accomplished. His quoted limiting flux is 10⁻¹⁰ cm⁻² sec⁻¹ sr⁻¹.

Hazen, Hodson, Winterstein, and Keller¹⁴ are using a very large cloud chamber, about 3 m² in area to look for $\frac{1}{3}e$ tracks, and quote a flux limit of 4 × 10⁻¹¹ cm⁻²sec⁻¹sr⁻¹. They have been de-

veloping artificial low-density tracks.

Evans *et al.*¹⁵ have used a different scheme to try to find $\frac{1}{3}e$ tracks. In a cloud chamber filled with helium at 28 atmospheres, they have looked (unsuccessfully) for tracks with large gaps between the drops. Their limit is 4 × 10⁻⁹ cm⁻² sec⁻¹ sr⁻¹ (with a 95% confidence level).

We have attempted gap counting using very narrow tracks in order to determine the number of primary interactions. However, there were unresolved problems because ions diffused along the track farther than expected.

McCusker¹ continued his original search, scanning an additional 1.3 times as much film as in his published work; he claimed no quark candidates beyond the original 5.

ACKNOWLEDGMENTS

A large number of people have gone far out of their way to help with this work. The Powell-Birge group at Lawrence Berkeley Laboratory aided throughout the program, particularly in getting us started. The PFR group at EGG, Las Vegas, was most helpful. Many Livermore people were indispensable, especially those in technical photography.

*Work performed under the auspices of the U. S. Atomic Energy Commission.

¹L. W. Jones, *Phys. Today* **26**, No. 5, 30 (1973); see also L. W. Jones, in *Proceedings of the Twelfth International Conference on Cosmic Rays, Hobart, 1971*, edited by A. G. Fenton and K. B. Fenton (Univ. of Tasmania Press, Hobart, Tasmania, 1971), p. 125.

²C. B. A. McCusker and I. Cairns, *Phys. Rev. Lett.* **23**, 658 (1969); I. Cairns, C. B. A. McCusker, L. S. Peak, and R. L. S. Woolcott, *Phys. Rev.* **186**, 1394 (1969).

³A. F. Clark, R. D. Ernst, H. F. Finn, G. G. Griffin, N. E. Hansen, D. E. Smith, and W. M. Powell, *Phys. Rev. Lett.* **27**, 51 (1971); D. E. Smith, N. E. Hansen, H. F. Finn, and A. F. Clark, *Bull. Am. Phys. Soc.* **17**, 603 (1972); A. F. Clark, H. F. Finn, N. E. Hansen, and D. E. Smith, *ibid.* **18**, 541 (1973).

⁴A. F. Clark, N. E. Hansen, and D. E. Smith, *Rev. Sci. Instrum.* **41**, 408 (1970).

⁵G. Griffin, Lawrence Livermore Laboratory Report No. UCRL-51371, 1973 (unpublished).

⁶C. E. Nielsen, thesis, University of California, Berkeley, 1941 (unpublished); *Phys. Rev.* **61**, 202 (1942).

⁷D. E. Smith, H. F. Finn, and D. W. Baltz, *Rev. Sci. Instrum.* **43**, 1239 (1972).

⁸*Studies in Penetration of Charged Particles in Matter*, Natl. Acad. Sci.-Natl. Res. Council. Publ. 1133 (1964).

⁹R. D. Ernst, Lawrence Livermore Laboratory Report No. UCRL-51214, 1972 (unpublished); R. D. Ernst, Lawrence Livermore Laboratory Report No. UCRL-51369, 1973 (unpublished).

¹⁰N. E. Hansen, Lawrence Livermore Laboratory Report No. UCID-16041, 1972 (unpublished).

¹¹J. A. Richards and L. W. Nordheim, *Phys. Rev.* **74**, 1106 (1948).

¹²R. N. Sternheimer and R. F. Peierls, *Phys. Rev. B* **3**, 3681 (1971).

¹³W. E. Hazen, *Phys. Rev. Lett.* **26**, 582 (1971).

¹⁴W. E. Hazen, A. L. Hodson, D. Winterstein, and O. Keller, in *Conference Papers, Thirteenth International Conference on Cosmic Rays, Denver, 1973* (University of Denver, Denver, 1973), Vol. 3, p. 2087, p. 2087.

¹⁵C. R. Evans, N. E. Fancey, J. Muir, and A. A. Watson, *Proc. R. Soc. Edinb. A* **70**, 143 (1972).

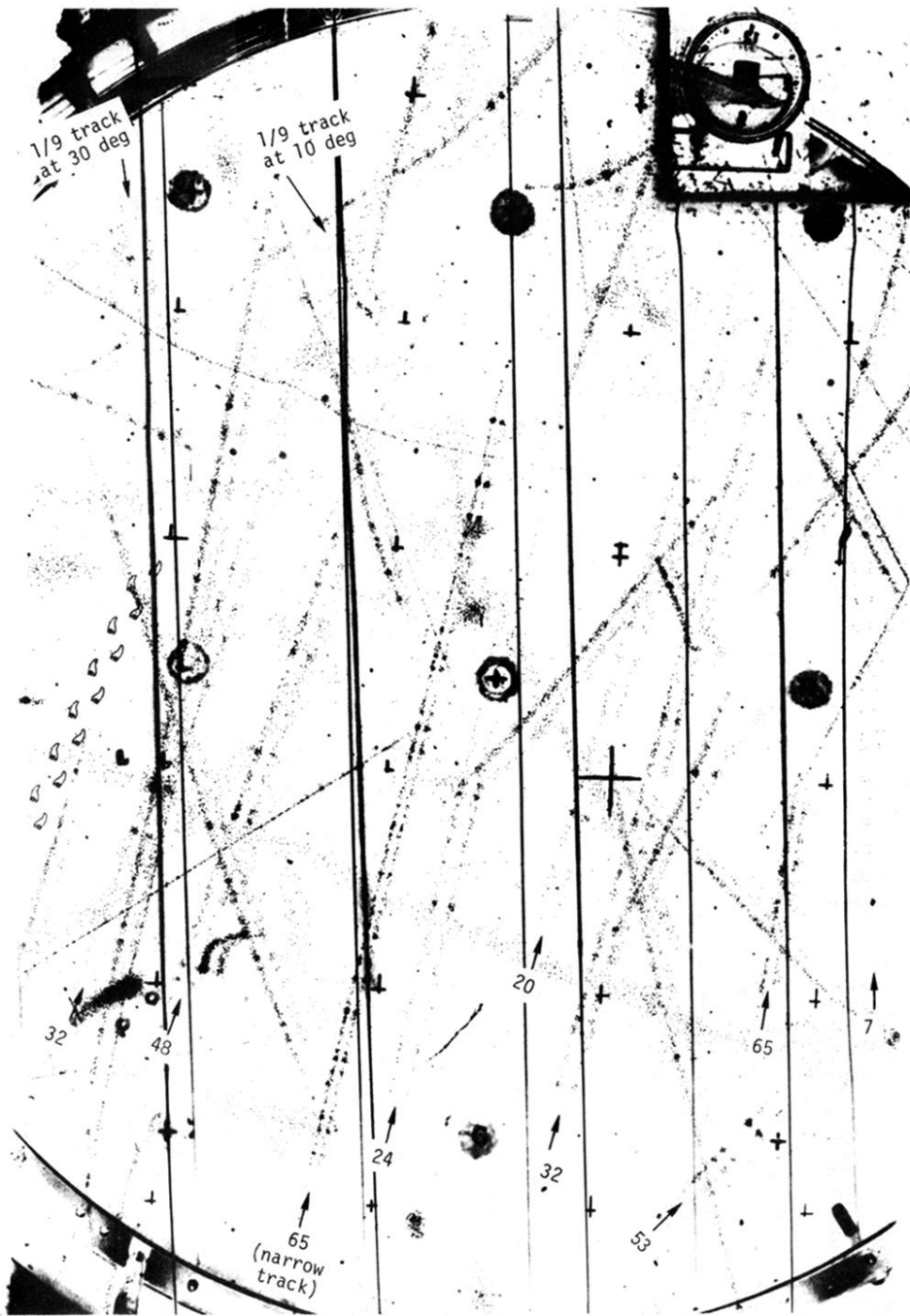


FIG. 1. An atypical photograph of a typical cloud chamber. The picture was taken looking approximately horizontally into a chamber; the zenith is at the top of the picture. There are 12 artificial tracks in this picture, indicating something of the variety of such tracks. The numbers in squares with arrows point along tracks made with a model to produce, on the average, the stated number of droplets per cm in the left-hand (positive) ion column. The 2 tracks in the upper left labeled $\frac{1}{9}$ are simulations of highly foreshortened tracks with $\frac{1}{9}$ normal density; the angles of the simulated $\frac{1}{9}$ -density tracks with the camera direction were 30° and 10° . The track at the left is also a "quark" track, i.e., it is formed with a droplet density of $\frac{1}{9}$ normal. This track should help convince people that one can be trained to detect certain kinds of tracks in the midst of much clutter. One can notice that the chamber was too hot (under-expanded) at the top because the negative (right-hand) ion columns of the real tracks are underdeveloped (almost absent), whereas the bottom of the cloud chamber was at the proper temperature with the negative columns about half as dense as the left-hand positive columns.

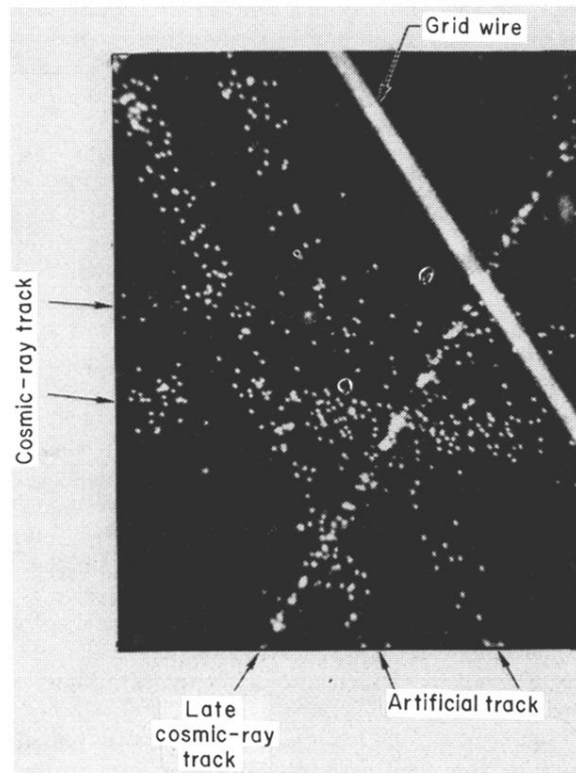


FIG. 2. Comparison of the droplets in normal and artificial tracks. The actual magnification from the reversal (2498) film is about 35 \times . The size of the droplets is determined by the resolution of the optics and the exposure of the film; the grid wire appears wide because it is so bright. The narrow single track arrived about 100 msec later than the cosmic-ray shower. Note the lack of background.